Hunting for renal protective phytoconstituents in *Artemisia judaica* L. and *Chrysanthemum coronarium* L. (Asteraceae)

Howaida I. Abd-Alla[a], Hanan F. Aly[b], Nagwa M. M. Shalaby[a], Marzougah A. Albalawy[d], Elsayed A. Aboutabl[c]

[a]Departments of Chemistry of Natural Compounds [b]Therapeutic Chemistry, National Research Centre, Giza [c]Pharmacognosy Department, Faculty of Pharmacy, Cairo University, Cairo, Egypt [d]Department of Chemistry, Faculty of Science, Tabuk University, Tabuk, Kingdom of Saudi Arabia

Correspondence to Howaida I. Abd-Alla, PhD, Department of Chemistry of Natural Compounds, National Research Centre, Dokki 12622, Giza, Egypt
Tel: +20 333 71615; fax: +20 233 70931;
e-mail: howaida_nrc@yahoo.com

Received 8 January 2014
Accepted 25 March 2014

Egyptian Pharmaceutical Journal
2014, 13:46–57

Aim

This study aimed to evaluate the potential renal protective activity of *Artemisia judaica* L. and *Chrysanthemum coronarium* L., belonging to family Asteraceae, collected in Mountains of Tabuk, Kingdom of Saudi Arabia. The ameliorative role of petroleum ether, ethyl acetate, and methanol successive extracts thereof on renal hyperlipidemic and hyperglycemic rats was studied. Active compounds isolated from the bioactive ethyl acetate extract of *A. judaica* were characterized and identified.

Material and methods

Hyperlipidemia and hyperglycemia were induced in rats. Evaluation of renal protection was carried out through determination of kidney biochemical markers and histopathological examination. Kidney disorder biomarkers (creatinine and total urea) as well as kidney marker enzyme (glyceraldehyde-3-phosphate dehydrogenase) activity were evaluated. Oxidant–antioxidant status in kidney was assessed by determination of glutathione, lipid peroxide, and nitric oxide. The free radical scavenging activity was performed using 1,1-diphenyl-2-picrylhydrazyl. The extract exhibiting the most significant bioactivity was investigated for its phytoconstituents.

Results and conclusion

Treatment with *A. judaica* successive extracts, in particular ethyl acetate, effectively ameliorated diabetic renal dysfunction more than those of *C. coronarium*. The results revealed improvement in all the investigated parameters, which was confirmed by kidney histopathological analysis. Phytochemicals in the most promising extract (ethyl acetate extract of aerial parts of *A. judaica*) were isolated and characterized through their physical, chemical, chromatographic, and spectral analyses (UV, MS, ^{1}H NMR, and ^{13}C NMR). One sesquiterpene lactone, vulgarin (**1**); three triterpenes, taraxerol acetate (**2**), β-amyrin (**3**), and lupeol (**4**); a phytosterol, β-sitosterol (**5**); and four flavonoids, lutoelin-3′-methyl ether (**6**) and its glycoside, luteolin 3′-methyl ether-7-glucoside (**7**), luteolin-6,7,4′-trimethyl ether (**8**), and artemetin (**9**), were identified. All compounds are reported for the first time in the investigated plant except **1**, **6**, and **7**. The bioactivity may be attributed to the terpenoidal and flavonoidal compounds.

Keywords:

Artemisia judaica L., *Chrysanthemum coronarium* L., flavonoids, renal protective, sesquiterpene lactone, triterpenes

Egypt Pharm J 13:46–57

1687-4315

Introduction

Hyperlipidemia is one of the major health problems because of the close correlation between cardiovascular diseases and lipid abnormalities [1]. Hyperglycemia results from abnormalities in insulin secretion and/or insulin action, both caused by impaired metabolism of glucose, lipids, and protein [2]. In hyperglycemic patients, impaired carbohydrates accelerate lipolysis, resulting in hyperlipidemia. Renal function tests (levels of creatinine and urea in the serum) are usually performed in hyperlipidemic–hyperglycemic rats to demonstrate the presence and/or absence of active lesion in the kidney, as well as to assess the normal functioning capacity of different parts of the functioning unit (nephron) [3]. Despite the presence of known antihyperglycemic pharmaceuticals, hyperglycemia and the related complications continue to be a major medical problem. Searching for new safe antihyperglycemic phytopharmaceuticals is still attractive [4,5].

Artemisia judaica L. and *Chrysanthemum coronarium* L. (Asteraceae) grow wildly in Tabuk region, northwestern part of Saudi Arabia. For many years, *A. judaica* and the edible *C. coronarium* have enjoyed a reputation among herb experts in Egypt and Saudi Arabia as traditional medicinal herbs. *A. judaica*, *Artemisia campestris*, and *Artemisia herba-alba* have been recommended for treatment of certain disorders [6,7]. In addition, the protective effect of *Chrysanthemum morifolum* on diabetic retinopathies in rats was reported [6]. It was, thus, deemed of interest to elucidate the ameliorative role of successive extracts (petroleum ether, ethyl

acetate, and methanol extracts) of each of *A. judaica* and *C. coronarium* on renal hyperlipidemic (fed a high fat diet) and hyperglycemic rats [induced by high fat diet and low doses of streptozotocin (STZ)], through measuring kidney marker tests and histopathological examination and to investigate the phytoconstituents of the promising bioactive extract.

Materials and methods

Plant material

The aerial parts (leaves and stems) of *A. judaica* L. were collected from Jabal Al-Louz (Almond Mountain) and of *C. coronarium* L. from mountain region of Alkurr Wadi, Tabuk area, Saudi Arabia in Spring 2011. The two plants were identified by Dr Amal M. Fakhri Abdelsalam, Plant Culture Biology Department, Tabuk University, Tabuk, Saudi Arabia. Voucher specimens are deposited in the herbarium, National Research Centre, Cairo (Egypt).

Animals

A total of 105 male Wister rats (8–12 weeks age, 110–120 g weight) provided by the Animal House of the National Research Centre were housed in a temperature-controlled environment (26–29°C), with a fixed light/dark cycle for 2 weeks to acclimatize; they were allowed free access to food and water *ad libitum* and randomly divided into seven groups of 15 animals each. This study was approved by the Ethical Committee of the National Research Centre.

Chemicals and reference material

High analytical grade chemicals from Sigma-Aldrich (St Louis, Missouri, USA), Merck (Darmstadt, Germany), BDH (Poole, UK), Riedel de Haën (Seelze, Germany), and Fluka (Buchs, Switzerland) were used. All solvents used for extraction and chromatographic separation were of analytical grade. The kits used were supplied by Biosystems (Barcelona, Spain) and Biodiagnostic Chemical Company (Giza, Egypt). Reference sterols and triterpenes were obtained from Merck.

Experimental design of bioactivity assays

Group 1 (normal control) received normal diet and water. Groups 2, 3, and 4 separately received orally normal diet with petroleum ether, ethyl acetate, and methanol extracts of *C. coronarium*, respectively. Groups 5, 6, and 7 separately received orally normal diet with petroleum ether, ethyl acetate, and methanol extracts of *A. judaica*, respectively. Group 8 [hyperlipidemia module associated with hyperglycemia (the HL-HG group)] received orally a high fat diet, cholesterol at a dose of 30 mg/0.3 ml/animal a week for 4 weeks [8], and were injected with STZ (35 mg/kg) [9] at the end of 4 weeks. Groups 9–14, the HL-HG group, were treated orally with the successive extracts of each plant. These extracts were separately, orally administered (500 mg/kg body weight) for 45 days [10]. The treatments were initiated after 3 days of STZ-induced diabetic state (glucose≥250 mg/dl) daily for 45 days. Group 15, the HL-HG group, received orally the standard antihyperlipidemic reference drug, fluvastatin at a dose of 20 mg/kg/day [11], and the antihyperglycemic reference drug, glibenclamide at a dose of 5 mg/kg daily for 45 days [12]. After 4 weeks of dietary manipulation of hyperlipidemic diet, the experimental rats were fasted overnight and intraperitoneally injected with freshly prepared solution of STZ. Serum glucose levels were estimated regularly every 3 days. Hyperglycemic rats were only considered for glucose level of at least 250 mg/dl. At the completion of the study, rats were fasted overnight, anesthetized with diethyl ether, and blood samples were collected. Serum was prepared by centrifugation and used for estimation of lipid profile. Rats were then killed and the kidney was rapidly removed, washed in saline, dried on filter paper, weighed, and homogenized in phosphate buffer for further biochemical analyses, and for histopathological examination kidney was fixed in 10% formalin solution.

Determination of kidney function tests

Creatinine was estimated by measuring the absorbance of the colored complex with picrate in an alkaline medium at 520 nm [13].

Total urea was measured colorimetrically (530–560 nm) applying the Berthelot reaction [14].

Kidney marker enzyme glyceraldehyde-3-phosphate dehydrogenase (GAPDH) was determined by enzyme-linked immunosorbent assay kit.

Oxidant–antioxidant status in kidney

It was assessed in the serum by determination of glutathione (GSH) (Biodiagnostic kits, Giza, Egypt) [15], lipid peroxide (malondialdehyde; MDA) [15], and nitric oxide (NO) [16].

Histopathological analysis

Kidney slices were fixed in 10% paraformaldehyde and embedded in paraffin wax blocks. Sections (5 m thick) were stained with hematoxylin and eosin (H&E) and examined under light microscope for determination of pathological changes [17].

DPPH radical scavenging activity

The antioxidant scavenging activity of serial concentrations of each ethyl acetate extract (10–1000 μg/ml) on 1,1-diphenyl-2-picrylhydrazyl (DPPH) free radical was carried out [18,19]. The decrease in optical density of DPPH was calculated with respect to control as follows:

$$\% \text{ Inhibition} = \frac{A_{control} - A_{Sample} \times 100}{A_{control}}.$$

Statistical analysis

Statistical analysis was carried out by one-way analysis of variance and Costat computer program (Cohort Software, Berkeley, CA) coupled with post-hoc (least significance difference). Unshared letters indicate significant correlation at *P* value of 0.05 or less.

Phytochemical investigation

Chromatographic techniques

Thin layer chromatography (TLC) was carried out on Silica gel 60 F_{254}-precoated aluminium plates (0.2 mm; Merck), and Whatman 1 mm sheets were used for paper chromatography (PC). Solvent systems – S_1, benzene/EtOAc (9.5 : 0.5); S_2, (8.5 : 1.5); and S_3, EtOAc/MeOH/H_2O/HOAc (16 : 2 : 0.5 : 0.5) – were used for TLC, whereas S_4, *n*-BuOH/HOAc/H_2O (4 : 1 : 5, top layer), and S_5, 15% aqueous HOAc, were used for PC. Spray reagents used were: R_1, sulphuric acid/methanol (30%), followed by heating at 105°C for 1–2 min for terpenes and sterol and R_2, 1 g powder of $AlCl_3$ in 100 ml of ethanol, for flavonoids. Column chromatography (CC) was carried out using silica gel (Si) 60 (E. Merck) and Sephadex LH-20 (Pharmacia Fine Chemicals AB, Uppsala, Sweden).

Apparatus

Electrothermal digital and Gallenkamp electrothermal melting point apparatus were used. UV–vis spectra were recorded on spectrophotometer model UV-240 (Shimadzu Corporation, Tokyo, Japan). EI-MS spectra were recorded on a Finnigan MAT 95 spectrometer (70 eV) (Finnigan MAT, San Jose, California, USA). NMR spectra were recorded at 300 (^{1}H) and 75 (^{13}C) MHz on Varian Mercury 300 (Varian, West Sussex, UK) spectrometer; δ values are reported as ppm relative to TMS in the convenient solvent and coupling constants *J* in Hz.

Extraction, fractionation, and isolation

The air-dried powdered aerial part of *A. judaica* L. and *C. coronarium*, 2.3 kg each, was individually, successively, and exhaustively extracted in Soxhlet extractor using solvents of increasing polarity in the following order: petroleum ether (40–60°C), ethyl acetate followed by methanol. The extracts were evaporated to dryness under vacuum. The solvent-free extractives of *A. judaica* (8.29, 60.44, and 25.93 g; yield 0.39, 2.63, and 1.12%, respectively) and of *C. coronarium* (25.44, 26.22, and 58.19 g; yield 2.28, 1.14, and 2.53%, respectively) were obtained.

The promising bioactive ethyl acetate extract of *A. judaica* was subjected to Si CC (5 × 120 cm, 650 g) with a gradient of ethyl acetate in *n*-hexane to give six main fractions (I–VI). Fraction I eluted with *n*-hexane/ethyl acetate (9 : 1) gave a white crystalline precipitate, which was recrystallized from methanol to yield compound **1** (27 mg). Fraction II (28.0 g) eluted with *n*-hexane/ethyl acetate (9 : 2) was rechromatographed on Si CC (400 g) and eluted with petroleum ether (40–60°C) followed by increasing proportions of toluene. Subfractions 7–18, eluted with petroleum ether/toluene (9 : 2), were further purified on Si CC, using the same eluent to afford compound **2** (14 mg). Subfractions 22–37, eluted with petroleum ether/toluene (7 : 3), gave pure compound **3** (5 mg) by crystallization in methanol. Fraction III, eluted with *n*-hexane/ethyl acetate (9 : 3), was resubjected to Si CC using the same eluent to afford compound **8** (18 mg) and compound **9** (22 mg). Fraction IV, eluted with *n*-hexane/ethyl acetate (9 : 4), was rechromatographed using petroleum ether/CH_2Cl_2 to afford compound **4** (22 mg). Fraction V, eluted with *n*-hexane/ethyl acetate (1 : 1), yielded compound **5** (35 mg) on recrystallization from methanol. Fraction VI, eluted with ethyl acetate only, was rechromatographed on Si columns using CH_2Cl_2/methanol (8 : 2) as eluent and further purified on Sephadex LH-20 (methanol as eluent) to give compounds **6** (20 mg) and **7** (11 mg). The purity of compounds was checked by comparative TLC and/or PC. Spots of flavonoids were visualized under UV light at 365 nm before and after exposure to ammonia vapor and detected by UV fluorescence after spraying with R_2. Terpenes and sterol were visualized by R_1.

The spectral data of the isolated compounds were illustrated as the following:

Compound **1**: white crystals; m.p.: 174–176°C; R_f: 0.52 (S_1); $C_{15}H_{20}O_4$; UV spectral data: λ_{max} (MeOH): 216 nm; MS: *m/z* (100%): 264 (M^+, 20.09); ^{1}H NMR (CD_3OD, 300 MHz): δ ppm 6.64 (1H, *d*, *J* = 10.2 Hz, H-3), 5.80 (1H, *d*, *J* = 10.2 Hz, H-2), 4.39 (1H, *dd*, *J* = 10.2, 11.2 Hz, H-6), 2.48 (1H, *d*, *J* = 11.2 Hz, H-5), 2.50 (1H, *q*, *J* = 6.8 Hz, H-11), 1.93 (2H, *m*, H-8α, H-9$_\beta$), 1.70 (1H, *m*, H-7), 1.60 (2H, *m*, H-8$_\beta$, H-9α), 1.51 (3H, *s*, CH_3-15), 1.26 (3H, *s*, CH_3-14), 1.20 (3H, *d*, *J* = 6.8 Hz, CH_3-13); ^{13}C NMR (CD_3OD, 75 MHz): δ ppm 204.6 (C-1), 181.9 (C-12), 155.1 (C-3), 125.0 (C-2), 80.5 (C-6), 71.0 (C-4), 55.5 (C-5), 54.1 C-7), 47.4 (C-10), 41.8 (C-11), 35.7 (C-9), 23.6 (CH_3-15), 23.4 (C-8), 20.6 (CH_3-14), 12.6 (CH_3-13).

Compound **2**: colorless needles; m.p.: 302–305°C; R_f: 0.94 (S_2), $C_{32}H_{52}O_2$; ^{1}H NMR ($CDCl_3$, 300 MHz): δ ppm 5.31 (1H, *m*, H-14), 4.49 (1H, *m*, H-3), 2.01 (3H, *s*, 3_β OAc), 1.07 (3H, *s*, CH_3-26), 0.95 (6H, *s*, CH_3-25/30), 0.93 (3H, *s*, CH_3-29), 0.91 (3H, *s*, CH_3-27), 0.87 (6H, *s*, CH_3-23/24), 0.83 (3H, *s*, CH_3-28); ^{13}C NMR ($CDCl_3$, 75 MHz): δ ppm 171.4 (CH_3 COO^-), 158.1 (C-14), 116.9 (C-15), 81.4 (C-3), 55.3 (C-5), 49.0 (C-9), 48.5 (C-18), 41.0 (C-19), 39.1 (C-8), 38.1 (C-1), 38.0 (C-13), 37.9 (C-4), 37.8 (C-10), 37.7 (C-22), 36.9 (C-12), 36.2 (C-17), 35.2 (C-21), 33.5 (C-16), 32.6 (CH_3-30), 33.4 (C-7), 29.5 (C-27/28), 28.8 (C-20), 28.0 (CH_3-23), 26.2 (CH_3-26), 23.9 (C-2), 22.4 (CH_3-29), 20.9 (CH_3COO^-), 18.4 (C-6), 18.0 (C-11), 16.5 (CH_3-24), 15.7 (CH_3-25).

Compound **3**: white crystalline needles; mixed m.p.: 196–197°C; R_f: 0.79 (S_1).

Compound **4**: white crystalline needles; m.p.: 211–212°C; R_f: 0.84 (S_2); $C_{30}H_{50}O$, UV spectral data: λ_{max} (MeOH): 210 nm; EIMS: *m/z* (%): 426 (M^+, 43.3), 411 (M^+–CH_3, 10.0), 218 (38.3), 207 (55.0), 203 (30.1), 189 (60.0), 177 (10.2), 121 (68.1), 95 (100), 69.0 (94.7); ^{1}H NMR ($CDCl_3$, 300 MHz): 4.70 and 4.54 (each 1H, *m*, CH_2-29), 3.24 (1H, *dd*, H-3), 2.42 (1H, *m*, H-19α), 1.94 (1H, *m*, H-21_β), 1.71 (3H, *s*, CH_3-30), 1.44 (1H, *m*, H-21_β), 1.02 (3H, *s*, CH_3-26), 0.97 (3H, *s*, CH_3-23), 0.96 (3H, *s*, CH_3-27), 0.92 (3H, *s*, CH_3-25), 0.88 (3H, *s*, CH_3-28), 0.84 (3H, *s*, CH_3-24); ^{13}C NMR ($CDCl_3$, 75 MHz): 150.8 (C-20), 109.0 (C-29), 79.4 (C-3), 55.2 (C-5), 50.1 (C-9), 48.2 (C-18), 47.9 (C-19), 42.8 (C-17), 42.7 (C-14), 41.3 (C-8), 40.4 (C-22), 38.9 (C-4), 38.7 (C-1), 38.0 (C-13), 37.4 (C-10), 35.9 (C-16), 34.2 (C-7), 29.7 (C-21), 27.6 (CH_3-23), 27.4 (C-2/5), 25.1 (C-12), 21.4 (C-11), 19.2 (CH_3-30), 18.2 (C-6), 17.7 (CH_3-28), 16.4 ($2CH_3$-25/26), 15.1 (CH_3-24), 14.2 (CH_3-27).

Compound **5**: white crystals; m.p.: 136–137°C; R_f: 0.53 (S_2); $C_{29}H_{50}O$; MS *m/z* (100%): 414 [M^+, 49.5], 415 [M^++H, 100], 399 [M^+–OH, 32.4], 397 [M^+–OH], 36.9], 330 (44.9), 302 (20.4), 273 (13.9), 255 (53.4), 231 (39.2), 312 (30.9); ^{1}H NMR ($CDCl_3$, 300 MHz): δ ppm 5.35 (1H, *d*, *J* = 5.4 Hz, H-6), 3.52 (*m*, H-3); ^{13}C NMR ($CDCl_3$, 75 MHz): δ ppm 140.6 (C-5), 121.7 (C-6), 71.5 (C-3), 56.7 (C-14), 56.4 (C-17), 50.4 (C-9), 46.1 (C-24), 42.0 (C-4/13), 39.9 (C-12), 37.4 (C-1), 36.7 (C-10), 36.4 (C-20), 34.4 (C-22), 32.1 (C-7/8), 31.9 (C-2), 29.4 (C-25), 28.0 (C-16), 26.4 (C-23), 24.0 (C-15), 23.4 (C-28), 21.3 (C-11), 20.2 (CH_3-26), 19.8 (CH_3-19), 19.4 (CH_3-27), 19.1 (CH_3-21), 12.1 (CH_3-29), 12.0 (CH_3-18).

Compound **6**: yellow powder; m.p.: 258–259°C; R_f: 0.89 (S_4); $C_{16}H_{12}O_6$; UV spectral data: λ_{max} (MeOH): 246, 268, 350, (+NaOMe): 265, 327, 412, (+$AlCl_3$): 277, 300, 363, 391, (+$AlCl_3$+HCl): 255.5, 272, 300, 354, (+NaOAc): 272, 357.5, (+ NaOAc+H_3BO_3): 276, 348 nm. MS *m/z* (100%): 300 [M^+, 100], 301 [M^++H, 33.4], 153 [A_1+H, 27.2], 152 [A_1^+, 7.2], 151, [B_1^+, 7.5]; ^{1}H NMR (DMSO-d_6, 300 MHz): δ ppm 12.95 (1H, *s*, OH-5), 7.56 (1H, *d*, *J* = 2.1 Hz, H-2′), 7.55 (1H, *dd*, *J* = 2.1, 5.4 Hz, H-6′), 6.95 (1H, *d*, *J* = 5.4 Hz, H-5′), 6.89 (1H, *s*, H-3), 6.57 (1H, *d*, *J* = 2.1 Hz, H-8), 6.22 (1H, *d*, *J* = 2.1 Hz, H-6), 3.89 (3H, *s*, OCH_3-3); ^{13}C NMR (DMSO-d_6, 75 MHz): δ ppm 181.7 (C-4), 164.0 (C-7), 163.6 (C-2), 161.4 (C-5), 157.3 (C-9), 150.7 (C-4′), 148.1 (C-3′), 121.5 (C-1′), 120.4 (C-6′), 115.7 (C-5′), 110.2 (C-2′), 104.4 (C-3), 103.5 (C-10), 98.8 (C-6), 94.1 (C-8), 56.3 (OCH_3-3′).

Compound **7**: yellow powder; m.p.: 174–176°C; R_f: 0.22 (S_4); $C_{15}H_{24}O_6$; UV λ_{max} (MeOH): 255, 270sh, 350, (+NaOMe): 266, 405 (+$AlCl_3$): 273, 300sh, 392, (+$AlCl_3$+HCl): 273, 298sh, 385, (+NaOAc): 268, 364, (+NaOAc+H_3BO_3): 268, 367 nm. MS *m/z* (100%): 300 [M^+, 100], 287 (14), 260 (22), 218 (10), 148 (7), 86 (25), 63 (8); ^{1}H NMR (DMSO-d_6, 300 MHz): δ ppm aglycone: 7.48 (1H, *dd J* = 8.1, 2.0 Hz, H-6′), 7.44 (1H, *d*, *J* = 2.0 Hz, H-2′), 6.88 (1H, *d*, *J* = 8.1 Hz, H-5′), 6.73 (1H, *s*, H-3), 6.76 (1H, *d*, *J* = 2.0 Hz, H-8), 6.47 (1H, *d*, *J* = 2.0 Hz, H-6), 3.92 (3H, *s*, OCH_3-3), glucose moiety 5.13 (1H, *d*, *J* = 6.9 Hz, H-1′).

Compound **8**: yellow crystals; m.p.: 197–198°C; R_f: 0.57 (S_3), $C_{18}H_{16}O_7$; UV spectral data: λ_{max} (MeOH): 214, 227, 344; (+NaOMe): 212, 234, 298, 400 nm; ^{1}H NMR ($CDCl_3$, 300 MHz): δ ppm 9.50 (OH-3′), 7.60 (1H, *dd*, *J* = 8.6, 2.3 Hz, H-6′), 7.58 (1H, *d*, *J* = 2.3 Hz, H-2′), 7.10 (1H, *d*, *J* = 8.6 Hz, H-5′), 6.92 (1H, *s*, H-8), 6.82 (1H, *s*, H-3), 3.94 (3H, *s*, OCH_3-7), 3.88 (3H, *s*, OCH_3-4′), 3.74 (3H, *s*, OCH_3-6);^{13}C NMR ($CDCl_3$, 75 MHz): δ ppm 182.2 (C-4), 163.9 (C-2), 158.7 (C-7), 152.6 (C-9), 152.2 (C-4′), 152.1 (C-5), 146.8 (C-3′), 131.9 (C-6), 123.0 (C-1′), 118.8 (C-6′), 113.1 (C-2′), 112.1 (C-5′), 105.1 (C-10), 103.4 (C-3), 91.6 (C-8), 60.0 (OCH_3-6), 56.4 (OCH_3-7), 55.8 (OCH_3-4′).

Compound **9**: yellow crystals; m.p.: 147°C; R_f: 0.68 (S_3); $C_{20}H_{20}O_8$; UV spectral data: λ_{max} (MeOH): 253, 275, 342; (+NaOMe): 253sh, 291, 332, 393sh; (+$AlCl_3$): 263, 283sh, 297sh, 372; (+$AlCl_3$+HCl): 261, 284, 359, 402sh; (+NaOAc): 254, 273, 343; (+NaOAc+H_3BO_3): 255, 273, 344 nm; EIMS: *m/z* (%): 388 (M^+, 100), 373 (64), 345 (13), 343 (16), 315 (8), 197 (4), 165 (39), 69 (62), 57 (64); ^{1}H NMR ($CDCl_3$, 300 MHz): δ ppm 7.72 (1H, *dd*, *J* = 8.5, 2.1 Hz, H-6′), 7.67 (1H, *d*, *J* = 2.1 Hz, H-2′), 6.97 (1H, *d*, *J* = 8.5 Hz, H-5′), 6.49 (1H, *s*, H-8), 3.96 (3H, *s*, OCH_3-3′), 3.96 (3H, *s*, OCH_3-4′), 3.95 (3H, *s*, OCH_3-7), 3.91 (3H, *s*, OCH_3-6), 3.85 (3H, *s*, OCH_3-

3); ^{13}C NMR ($CDCl_3$, 75 MHz): δ ppm 178.9 (C-4), 158.8 (C-7), 155.8 (C-2), 152.8 (C-9), 152.3 (C-5), 151.4 (C-4′), 148.9 (C-3′), 138.9 (C-3), 132.4 (C-6), 123.8 (C-1′), 122.2 (C-6′), 111.5 (C-5′), 110.0 (C-2′), 105.7 (C-10), 90.4 (C-8), 60.8 (OCH_3-3), 60.1 (OCH_3-6), 56.3 (OCH_3-7), 56.2 (OCH_3-4′), 56.0 (OCH_3-3′).

Results

Determination of kidney function tests

The results demonstrated insignificant change in serum total urea, creatinine, and GAPDH in normal treated rats with successive extracts of each of *C. coronarium* and *A. judaica* (Table 1). In contrast, hyperlipidemic–hyperglycemic rats showed significant elevation in total urea and creatinine, whereas kidney marker enzyme GAPDH was significantly decreased. Treatment of hyperlipidemic–hyperglycemic rats with the successive extracts of *C. coronarium* showed insignificant change in total urea and creatinine with levels nearly reaching control and lesser degree of improvement in GAPDH compared with control. Furthermore, marked improvement was noticed in total urea, creatinine, and GAPDH levels as a result of treatment of hyperlipidemic–hyperglycemic rats with all extracts of *A. judaica*, with percent reaching 271.32, 354.50, and 47.45%, respectively, for petroleum ether, 273.65, 355.45, and 49.10%, respectively, for ethyl acetate, and 264.35, 336.36, and 26.56%, respectively, for methanol successive extract.

Table 1 The level of creatinine, total urea, and kidney marker enzyme, glyceraldehyde-3-phosphate dehydrogenase enzyme, activity in normal and different therapeutic groups

Group	Parameters		
	Creatinine (mg/dl)	Total urea (mg/dl)	GAPDH (ng/ml)
Negative control	1.10 ± 0.09[a]	43.23 ± 2.96[a]	8.07 ± 0.14[a]
PE extract of *A. judaica*	1.10 ± 0.09[a]	38.01 ± 1.76[a]	8.19 ± 0.16[a]
EA extract of *A. judaica*	0.70 ± 0.01[a]	31.22 ± 2.88[a]	8.22 ± 0.19[a]
M extract of *A. judaica*	0.80 ± 0.01[a]	34.24 ± 4.00[a]	8.00 ± 0.11[a]
PE extract of *C. coronarium*	0.72 ± 0.02[a]	31.10 ± 2.45[a]	8.10 ± 0.15[a]
EA extract of *C. coronarium*	0.70 ± 0.01[a]	34.34 ± 2.78[a]	8.04 ± 0.13[a]
M extract of *C. coronarium*	1.00 ± 0.05[a]	36.04 ± 0.88[a]	8.00 ± 0.13[a]
Positive control (HL-HG rats)	4.80 ± 0.09[b]	145.67 ± 5.90[c]	3.89 ± 0.67[d]
HL-HG+PE extract of *A. judaica*	0.90 ± 0.10[a]	29.00 ± 0.02[a]	7.72 ± 0.72 [a]
HL-HG+EA extract of *A. judaica*	1.10 ± 0.02[a]	32.40 ± 2.00[a]	6.92 ± 0.14[a]
HL-HG+M extract of *A. judaica*	0.89 ± 0.02[a]	28.31 ± 1.87[a]	7.85 ± 0.40[a]
HL-HG+PE extract of *C. coronarium*	0.93 ± 0.15[a]	37.66 ± 2.51[a]	7.05 ± 0.40[a]
HL-HG+EA extract of *C. coronarium*	0.96 ± 0.05[a]	34.22 ± 1.00[a]	5.12 ± 0.02[e]
HL-HG+M extract of *C. coronarium*	0.96 ± 0.05[a]	31.11 ± 10[a]	6.98 ± 0.13[a]
HL-HG+fluvastatin	1.00 ± 0.04[a]	37.33 ± 3.10[a]	7.10 ± 0.90[a]
HL-HG+glibenclamide	1.13 ± 0.06[a]	33.00 ± 1.90[a]	6.87 ± 1.10[a]

Data are expressed as mean ± SD of 10 rats in each group. *A. judaica*, *Artemisia judaica*; *C. coronarium*, *Chrysanthemum coronarium*; EA, ethyl acetate; GAPDH, glyceraldehyde-3-phosphate dehydrogenase; HL-HG, hyperlipidemic–hyperglycemic; M, methanol; PE, petroleum ether. Statistical analysis was carried out by one-way analysis of variance, and Costat computer program coupled with post-hoc (least significance); Unshared letters indicate significant differences at $P \leq 0.05$.

Oxidant — antioxidant status in kidney

Results in Table 2 indicate insignificant change in the kidney oxidative stress markers – MDA, GSH, and NO levels – in normal rats treated with the successive extracts of both *A. judaica* and *C. coronarium* as compared with the normal control group. Hyperlipidemic–hyperglycemic rats showed significant depletion in GSH, with significant increase in kidney MDA and NO as compared with the normal control group. Treatment of hyperlipidemic–hyperglycemic rats with successive extracts of both *A. judaica* and *C. coronarium* showed more pronounced amelioration in the mentioned antioxidant parameters than fluvastatin and glibenclamide standard drugs.

Histopathological examination

This examination of normal rat kidney showed normal cell structure and normal orientation of nephrons with adequate glomeruli and well-spaced tubules and no inflammation, no necrosis, no congestion, with well-presented cytoplasm (Fig. 1). Light microscopy of the renal cortex and medulla of hyperlipidemic–

Figure 1

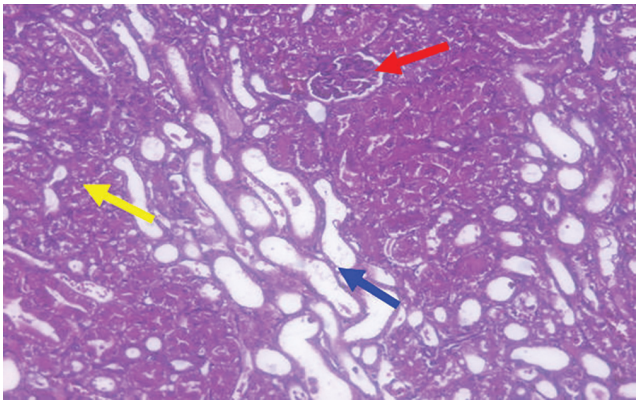

Normal control kidney section showing normal orientation of nephrons with adequate glomeruli and well-spaced tubules (H&E, × 100).

hyperglycemic rats revealed lesion and showed tubular necrosis, atrophy, dilatation, moderate interstitial edema, and interstitial inflammatory cell infiltrates. Glomeruli showed moderate proliferation of mesangial cells and matrix of glomeruli and hyaline thickening of some arteriole (Fig. 2a and b).

The histological examination of all successive extracts of *A. judaica*-treated hyperlipidemic–hyperglycemic rats showed no mesangial cells and matrix of glomeruli. Mild/negative tubular dilatation atrophy, focal interstitial edema, and mild interstitial inflammatory cell infiltrate were also seen (Figs 3–5, respectively).

In addition, all successive extracts of *C. coronarium*-treated hyperlipidemic–hyperglycemic rats showed histopathological observation characterized by mild/negative tubular atrophy, dilatation, interstitial edema, and interstitial inflammatory cell infiltrates. However, glomeruli showed focal proliferation of mesangial cells, matrix of glomeruli, and hyaline thickening of some arteriole (Figs 6–8, respectively).

DPPH radical scavenging activity

The DPPH free radical scavenging effects of each plant ethyl acetate extract is shown in Fig. 9. The tested extracts show appreciable free radical scavenging activities. *A. judaica* crude extract exhibited stronger radical scavenging activity than *C. coronarium* at different concentrations in a dose-dependent relationship; the activity increased as the concentration of tested plants extract increased. *A. judaica* and *C. coronarium* crude extracts were able to reduce the

Figure 2

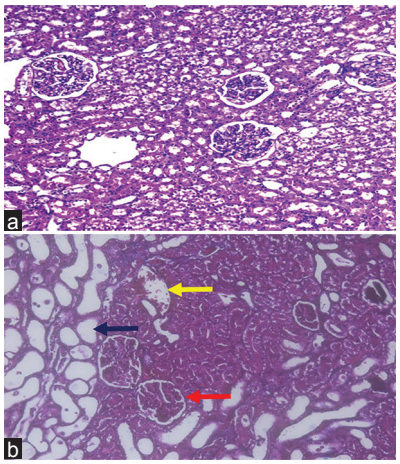

(a) The hyperlipidemic–hyperglycemic group showed proliferation of mesangial cells and matrix of glomeruli (red arrow); tubular atrophy (yellow arrow); and tubular dilatation (blue arrow) (H&E, × 200). (b) The hyperlipidemic–hyperglycemic group showed proliferation of mesangial cells and matrix of glomeruli (red arrow); thickened arteriole (yellow arrow); and tubular dilatation (blue arrow) (H&E, × 200).

Table 2 Glutathione concentration, lipid peroxide and nitric oxide levels in normal, hyperlipidemic–hyperglycemic and treated groups

Groups	Parameters		
	GSH (mg/g tissue)	NO (μmol/g tissue)	LPO (nmol/g tissue)
Negative controls	0.53 ± 0.09^{a}	18.16 ± 4.55^{c}	7.09 ± 1.54^{b}
PE extract of *A. judaica*	0.58 ± 0.07^{a}	16.99 ± 2.97^{c}	6.16 ± 1.12^{b}
EA extract of *A. judaica*	0.54 ± 0.02^{a}	20.11 ± 5.23^{c}	6.98 ± 0.80^{b}
M extract of *A. judaica*	0.59 ± 0.06^{a}	18.00 ± 2.14^{c}	6.13 ± 0.94^{b}
PE extract of *C. coronarium*	0.50 ± 0.05^{a}	14.39 ± 3.47^{c}	6.36 ± 1.35^{b}
EA extract of *C. coronarium*	0.55 ± 0.04^{a}	20.48 ± 6.82^{c}	6.18 ± 0.86^{b}
M extract of *C. coronarium*	0.59 ± 0.03^{a}	18.00 ± 3.15^{c}	7.00 ± 1.00^{b}
Positive control (HL-HG rats)	0.19 ± 0.02^{d}	74.24 ± 6.92^{f}	18.17 ± 0.96^{e}
HL-HG+PE extract of *A. judaica*	0.57 ± 0.03^{a}	22.13 ± 2.54^{c}	8.90 ± 1.10^{b}
HL-HG+EA extract of *A. judaica*	0.50 ± 0.02^{a}	25.16 ± 3.50^{c}	9.20 ± 0.56^{b}
HL-HG+M extract of *A. judaica*	0.59 ± 0.10^{a}	17.15 ± 3.14^{c}	7.06 ± 0.42^{b}
HL-HG+PE extract of *C. coronarium*	0.54 ± 0.08^{a}	24.23 ± 6.94^{c}	8.71 ± 1.27^{b}
HL-HG+EA extract of *C. coronarium*	0.58 ± 0.12^{a}	27.26 ± 4.55^{c}	9.08 ± 0.49^{b}
HL-HG+M extract of *C. coronarium*	0.49 ± 0.01^{a}	18.17 ± 4.54^{c}	8.86 ± 0.72^{b}
HL-HG+fluvastatin	0.40 ± 0.01^{a}	27.26 ± 4.55^{c}	9.08 ± 0.49^{b}
HL-HG+glibenclamide	0.37 ± 0.02^{a}	31.81 ± 4.54^{c}	9.42 ± 0.52^{b}

Data are expressed as mean ± SD of 10 rats in each group. *A. judaica*, *Artemisia judaica*; *C. coronarium*, *Chrysanthemum coronarium*; EA, ethyl acetate; GSH, glutathione; HL-HG, hyperlipidemic–hyperglycemic; LPO, lipid peroxide; M, methanol; NO, lipid peroxide; PE, petroleum ether. Statistical analysis was carried out by one-way analysis of variance, and Costat computer program coupled with post-hoc (least significance); Unshared letters indicate significant differences at $P \leq 0.05$.

Figure 3

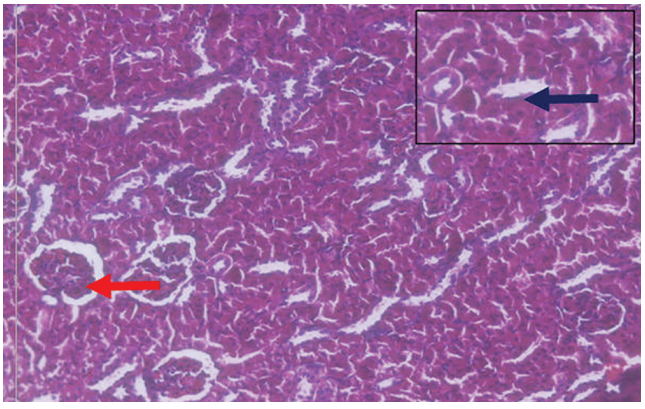

PE successive extract of *Artemisia judaica*-treated hyperlipidemic–hyperglycemic rats showed no mesangial cells and matrix of glomeruli (red arrow) and tubular dilatation (blue arrow) (H&E, × 200). PE, petroleum ether.

Figure 4

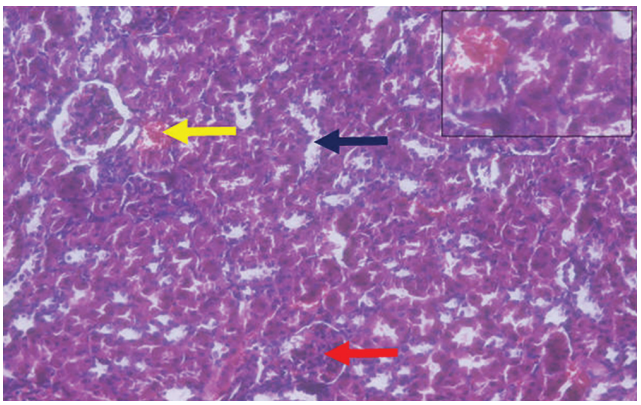

EA extract of *Artemisia judaica*-treated hyperlipidemic — hyperglycemic rats showed focal proliferation of mesangial cells and matrix of glomeruli (red arrow); thickened arteriole (yellow arrow); and tubular dilatation (blue arrow) (H&E, × 200). EA, ethyl acetate.

Figure 5

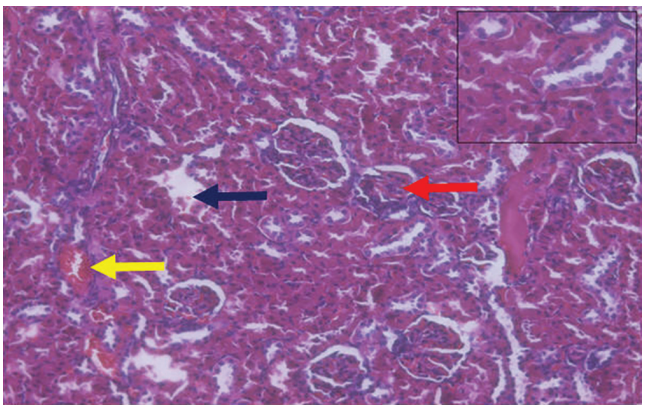

M extract of *Artemisia judaica*-treated hyperlipidemic — hyperglycemic rats showed focal proliferation of mesangial cells and matrix of glomeruli (red arrow); thickened arteriole (yellow arrow); and tubular dilatation (blue arrow) (H&E, × 200). M, methanol.

Figure 6

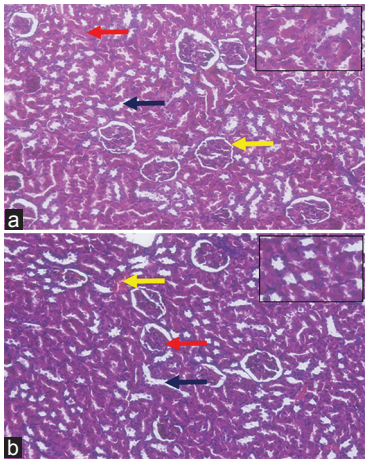

(a) PE extract of *Chrysanthemum coronarium*-treated hyperlipidemic–hyperglycemic rats showed focal proliferation of mesangial cells and matrix of glomeruli (red arrow); thickened arteriole (yellow arrow); and tubular dilatation (blue arrow) (H&E, × 200). (b) PE extract of *C. coronarium*-treated rats showed normal mesangial cells and matrix of glomeruli (red arrow); focal thickened arteriole (yellow arrow); and tubular dilatation (blue arrow) (H&E, × 200). PE, petroleum ether.

Figure 7

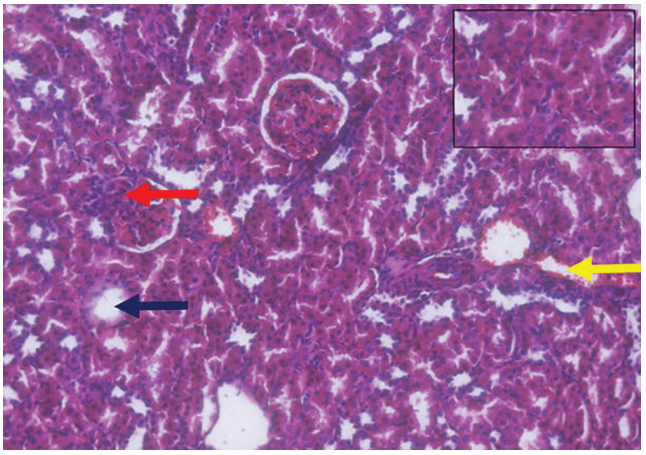

EA extract of *Chrysanthemum coronarium*-treated hyperlipidemic–hyperglycemic rats showed focal proliferation of mesangial cells and matrix of glomeruli (red arrow); thickened arteriole (yellow arrow); and tubular dilatation (blue arrow) (H&E, × 200). EA, ethyl acetate.

stable radical DPPH to the yellow color 1,1-diphenyl-2-picrylhydrazyl to give significant inhibitory percent 48.70 ± 0.80, 65.56 ± 0.57, 68.49 ± 0.89, 79.52 ± 0.59, and 82.89 ± 0.90% at concentration of inhibitor 10, 50, 100, 500, and 1000 µg/ml, respectively, for *A. judaica* crude extract. However, *C. coronarium* crude extract showed reducing inhibitory power of DPPH amounted 29.41 ± 0.80, 46.50 ± 6.67, 64.78 ± 5.96, 77.37 ± 6.17, and 80.78 ± 7.99% at the concentrations of extracts 10–1000 µg/ml, respectively. The dosage of extracts is expressed in µg of dry weight of the extract per ml of the assay mixture. DPPH is expressed as percentage. Data are represented as mean ± SD of three replicates.

Discussion

The antihyperglycemic effects of certain plants are attributed to their ability to restore the function of pancreatic tissues by causing an increase in insulin output or inhibiting the intestinal absorption of glucose or to facilitate metabolites in insulin-dependent processes [20]. Certain bioactive flavonoids and terpenes constituents are frequently implicated as having antihyperglycemic effect [8].

The present study indicated significant increase in serum urea and creatinine, accompanied with significant decrease in kidney marker enzyme GAPDH in hyperlipidemic–hyperglycemic rats. Increased concentrations of creatinine and total urea in blood during renal diseases or renal damage may be due to high

Figure 8

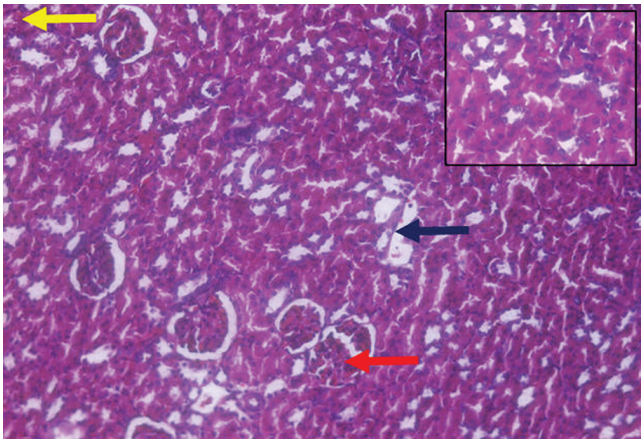

M extract of *Chrysanthemum coronarium*-treated hyperlipidemic–hyperglycemic rats showed focal proliferation of mesangial cells and matrix of glomeruli (red arrow); thickened arteriole (yellow arrow); and tubular dilatation (blue arrow) (H&E, × 200). M, methanol.

Figure 9

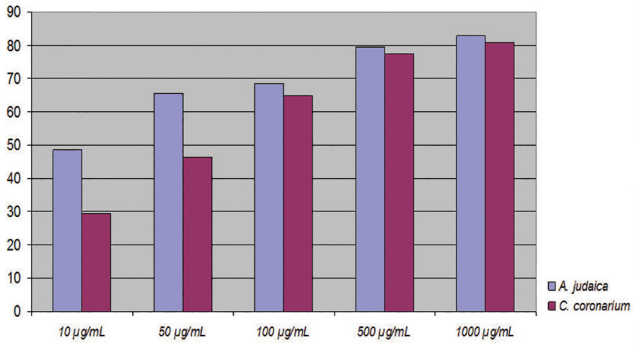

Percentage of DPPH inhibition induced by crude extract of *Artemisia judaica* L. and *Chrysanthemum coronarium* L. DDPH, 1,1-diphenyl-2-picrylhydrazyl.

activities of xanthine oxidase, lipid peroxidation, and increased triacylglycerol and cholesterol levels, as well as impairment of the urea cycle enzyme activities [3]. As the retention of creatinine in blood is an evidence of kidney impairment [21,22], the reduced levels of creatinine in serum (Table 1) imply that both plant extracts had interfered with creatinine metabolism and its eventual excretion from blood. The significant decrease in urea and creatinine may be explained on the basis of hypercholesterolemia in diabetic rats. One of the mechanisms that might be activated and hinder renal vascular function is oxidative stress [23]. It has been shown that rats consuming a high fat diet develop hyperlipidemia with elevations in renal lipid peroxidation products [24]. GAPDH is a key enzyme in glycolysis and is considered as the sensitive kidney function enzyme marker and was found to decrease in renal dysfunction [25].

Degradation of oxidized or oxidatively modified proteins is an essential part of the antioxidant defenses of cells. 4-Hydroxy-2-nonenal (HNE), a major reactive aldehyde formed by lipid peroxidation, causes many types of cellular damage [25]. HNE is considered to be the ultimate mediator of the toxic effects elicited by oxidative stress, as it is largely responsible for many types of cellular damage. HNE inactivates several enzymes, including GAPDH [25]. Binding of HNE to proteins can cause conformational changes and amino acid modifications, as well as the accumulation and aggregation of proteins causing cellular dysfunctions. The breakdown of such modified proteins is an essential defense mechanism against oxidative stress in cells [2]. The amount of GAPDH and its localization significantly affect the cell condition. Thus, GAPDH is considered as the sensitive enzyme marker catalyzing kidney function and was found to decrease in renal dysfunction [25]. Therefore, it is easy to imagine that degradation of HNE-modified GAPDH is crucial for the status of cells [26].

Hyperglycemia increased the generation of free radicals by glucose auto-oxidation and the increment of free radicals may lead to liver cell damage. The increase in oxygen free radicals in diabetic rats could be primarily due to the increase in blood glucose levels and secondarily due to the effect of the hyperglycemic agent, STZ [27]. Several plant constituents are known to reduce urea and creatinine levels as they usually increase in the serum of hyperglycemic rats [28].

Attention now is being focused on the increased oxygen consumption per nephron as a consistent tubule adaptation that occurs with nephron loss.

Hyperlipidemia–hyperglycemia state leads to the formation of free radicals. Too many reactive oxygen species and free radicals exhaust antioxidation factors, such as GSH and superoxide dismutase antioxidant enzyme, and shift the dynamic balance between oxidation and reduction. Oxidative stress can cause liver damage and lipid peroxidation and produce lots of intermediate products with reactivity and cytotoxicity that can lead to the necrosis or apoptosis of cells. Oxidative stress can also produce an inflammatory reaction through cell injury, causing the infiltration of the liver parenchyma by inflammatory cells [29].

GSH plays critical role in the detoxification process against reactive nitrogen species – for example, NO, NO_2, and ONOO [30]. Oxidized glutathione (GSSG) is formed by the linking of two tripeptides by disulfide bridge. The generation of GSSG takes place during the oxidation of GSH by glutathione peroxides to maintain the sufficient level of GSH. The increased

oxidized GSH levels in hyperlipidemic–hyperglycemic rats can be attributed to spontaneous nonenzymatic GSH oxidation as has been suggested by Harrison [31]. There is also increasing evidence to support the idea that the antioxidant activity of both plant successive extracts can play a very important role in the treatment of hyperlipidemia–hyperglycemia case in rats. Studies have shown that antioxidant therapy attenuates elevations in lipid peroxidation products [24]. The plant extracts may have reduced lipid peroxidation by acting as antioxidants, and hence aiding the endogenous antioxidant enzymes (such as superoxide dismutase, GSH peroxidase, and catalase) involved in the scavenging/inactivation of the reactive oxygen species or redox metal ions before lipid peroxidation takes place [32]. *A. judaica* and *C. coronarium* contain different phenolic compounds known as its major antioxidants [33–35]. Kim *et al*. [36] suggested that the possible mechanism of antihyperglycemic action by aqueous extracts from *C. coronarium* could be related to antioxidants that aid to recover from impaired metabolism of glucose. The present results indicate that both *A. judaica* and *C. coronarium* crude extracts exhibited strong DPPH free radical inhibitory effect at a dose-dependent response relationship at concentration of inhibitors 10–1000 μg/ml. *A. judaica* showed promising DPPH scavenging activity than *C. coronarium*. Several Artemisia and Chrysanthemum spp. – *A. herba-alba* Asso, *Artemisia vulgaris*, *Artemisia minor*, *Artemisia scoparia*, *Artemisia princeps*, *Artemisia asiatica*, *C. coronarium*, and *Chrysanthemum sinense* contain bioactive phenolics. The phenolics, mainly flavonoid constituents, generally play an important role in decreasing lipid peroxidation and oxidative stress of diseased animals [37]. The effect of *A. campestris* on renal impairment and oxidative stress in STZ-induced diabetic rats was reported [7]. The antioxidant and free radical scavenging activities of *Artemisia gmelinii* were found to relate to the phenolic compounds [33].

Total flavonoids from *Chrysanthemum morifolium* suggested improving antioxidant defense system, reversing lipid peroxidation, and protecting brain, liver, and kidney against lead-induced oxidative damage significantly [38].

In a recent study [35], we have investigated *C. coronarium* aerial parts for their phytochemical composition. This study revealed the isolation of three flavone aglycones and three flavonoid glycosides. The flavonoid aglycones, 5,7-dihydroxy-3,6,4′-trimethoxyflavone and scutellarin-6,7-dimethyl ether, were isolated from ethyl acetate extract. In addition, a new flavonoid glycoside, apigenin-7-*O*-[2′′(6′′′-*O*-β-D-acetylglucopyranosyl)]-6′′-*O*-acetylglucopyranoside, along with two known flavonoid glycosides, apigenin-7-*O*-(2′′-*O*-β-D-glucopyranosyl)-β-D-glucopyranoside and 6-methoxy qurecetin-7-*O*-β-D-glucopyranoside, were isolated from the methanol extract. These compounds may be responsible for the hypolipidemic and hypoglycemic effect of *C. coronarium*.

Phytochemical investigation

The bioactive extract, ethyl acetate of *A. judaica*, was phytochemically investigated. One sesquiterpene lactone, vulgarin (**1**); three terpenoidal compounds, taraxerol acetate (**2**), β-amyrin (**3**), and lupeol (**4**); one sterol, β-sitosterol (**5**), in addition to a flavone aglycone, lutoelin-3′-methyl ether (**6**), and its glycoside, luteolin 3′-methyl ether-7-glucoside (**7**); two polymethoxy flavones, luteolin-6,7,4′-trimethyl ether (**8**) and artemetin (**9**), were identified. Characterization of these compounds (Fig. 10) was achieved through their physical, chemical, chromatographic, and spectral analyses (UV, MS, ^{1}H NMR, and ^{13}C NMR). The analytical data were in agreement with those reported in the literatures [39–42].

Figure 10

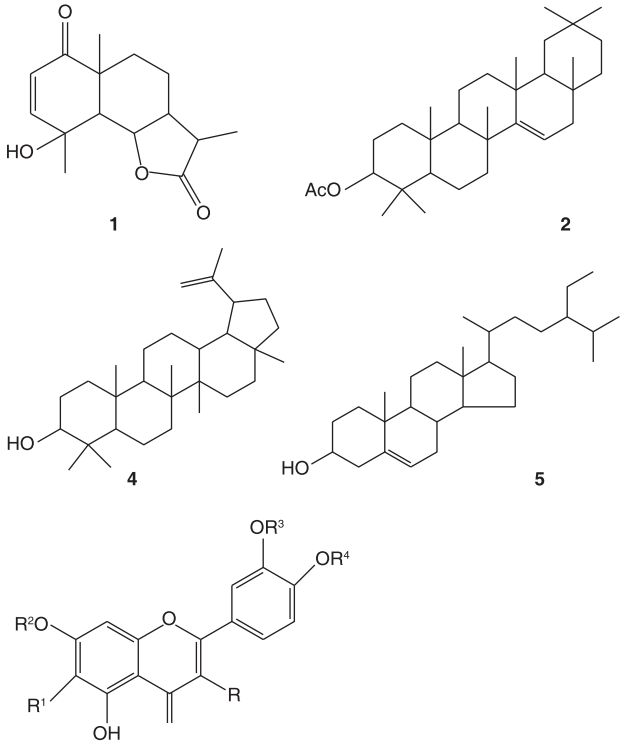

Compound	R	R^1	R^1	R^3	R^4
6	H	H	H	CH_3	H
7	H	H	Glc	CH_3	H
8	H	OCH_3	CH_3	H	CH_3
9	OCH_3	OCH_3	CH_3	CH_3	CH_3

Chemical structures of the isolated compounds from *Artemisia judaica* aerial parts.

UV spectral data compound **1** showed λ_{max} at δ 218 nm, which referred to its sesquiterpene lactone nature. ^{1}H NMR showed doublet absorption at δ 6.64 and 5.80 ppm, which related to H-3 and H-2, respectively, with J = 10.2 Hz. Proton at δ 2.48 ppm of H-5 appeared as doublet with J = 11.2 Hz and proton H-6 at δ 4.39 appeared as *dd* (J = 10.2, 11.2 Hz). ^{1}H-^{1}H COSY showed H–H coupling between the following: (3, 2), (6, 5), (6, 7), (11, 13), and methylene coupling (9_{β}, 9α), (9_{β}, 8_{β}), (8_{β}, 9α), (8α, 9_{β}), (9α, 8α), and (8α, 8_{β}). HQMC showed $^{2}J_{C-H}$ between secondary C and H. The compound was identified as 4α-hydroxy-1-oxo-5α,11β-H-eudesm-2-en-6α,12-olide (vulgarin). ^{1}H NMR spectrum of compound **2** showed eight sharp singlets at δ 1.07, 0.95 × 2, 0.93, 0.91, 0.87 × 2, and 0.83 ppm assigned to the protons of tertiary methyl groups at C-26, C-25, C-30, C-29, C-27, C-23, C-24, and C-28, respectively. A sharp singlet at δ 2.01 ppm corresponding to the methyl of acetate group and a peak at δ 5.31 ppm assigned to H-14 characteristic for the presence of a double bond at C-14 and C-15. ^{13}C NMR showed 32 sharp signals; those appearing at δ 32.6, 29.5 × 2, 28.0, 26.2, 22.4, 16.5, and 15.7 ppm were assigned to carbons of the methyl group at C-30, C-27, C-28, C-23, C-26, C-24, and C-25. A signal at δ 20.9 ppm was assigned to the methyl of the acetyl group and at δ 171.4 ppm for the carbonyl group of the acetyl radical. Compound **2** was identified as taraxerol acetate by comparison with published data [43,44]. Compound **3** was identified as β-amyrin through m.p., mixed m.p., and comparative TLC with authentic sample [44]. ^{1}H NMR spectrum of compound **4** showed seven sharp singlets at δ 1.71, 1.02, 0.97, 0.96, 0.92, 0.88, and 0.84 ppm assigned to the protons of tertiary methyl groups at C-30, C-26, C-23, C-27, C-25, C-28, and C-24, respectively. The two multiplets at δ 4.70 and 4.54 ppm could be ascribed to a methylene group at C-29. The compound was identified as lupeol confirmed by cochromatography with authentic sample and comparison with published data [43,45]. Compound **5** showed doublet absorption at δ 5.35 ppm of H-6 referred to the presence of double bond at C-5 and C-6 by constant δ of J = 5.4 Hz. In addition, a multiplet at δ 3.52 ppm represented H-3 surrounded by OH-β. ^{13}C NMR showed the presence of 29 carbons, two of which have chemical shift at δ 140.76 (C-5) and 121.7 ppm (C-6), representing the double bond at position 5 and 6. In addition, absorption represented carbon attached by OH (C-3) at value δ 71.5 ppm. The compound was identified as β-sitosterol [43]. Compounds **6–9** gave a positive ferric chloride test for phenolic hydroxyl groups and had UV absorption bands with maxima in the range of 240–285 and 300–550 nm, which agrees with the structure of flavones derivative [39].

Flavonoidal compounds **6–8** were expected to be luteolin derivatives on the basis of their chromatographic properties. UV spectra in methanol gave characteristic band I (at λ_{max} 342–350 nm) of luteolin nucleus. The absence of bathochromic shift in band II after addition of NaOAc spectrum indicated a substituted 7-OH group in the compounds **7–9** [39], whereas compound **6** exhibited bathochromic shift (~7.5 nm) indicating the presence of free 7-OH. The lack of bathochromic shift in NaOAc/H_3BO_3 spectrum for compounds **6–9** indicates the absence of *ortho* dihydroxy groups at ring B. A bathochromic shift of band I and band II induced by $AlCl_3$ and $AlCl_3$/HCl indicated the existence of 5-OH for compounds **6–9**, which also confirmed the absence of *ortho* dihydroxy groups at ring B. The bathochromic shift induced in NaOMe spectrum for band II together with its increased intensity indicates the presence of 5,7-dihydroxy groups observed in compound 6. For compounds **6** and **7**, the NaOMe spectrum showed a bathochromic shift without decrease in the intensity, which indicate to the presence of OH-4′ [39]. ^{1}H NMR spectra of compounds **6–9** showed an ABX system at δ ~7.72–7.44 ppm assigned for H-2′ and H-6′ and at ~7.10–6.88 ppm for H-5′, characterizing a 3′,4′-disubstituted B-ring. In addition, a singlet at ~6.13–6.89 ppm was assigned for H-3 indicating the aglycone moiety in compound luteolin for compounds **6–8** [40,46]. Compound **7** showed two doublets (J = 2.1 Hz) each integrated to one proton of an AX system of H-6 and H-8. The downfield of H-6 and H-8 (~+Δ0.2) in the spectrum of **7** relative to those of **6**, along with one β-anomeric proton signal at doublet 5.13 ppm (J = 6.9 Hz) was an evidence of the presence of a sugar moiety at 7-position [40]. Inspection of the ^{13}C NMR chemical shifts of compounds **8** and **9** clearly reveals the effect of the methylation of the phenolic hydroxyl at C-7 and the effect of the methoxy group at C-3. Thus, going from compounds **9** and **8** to compound **6**, the methylation effect causes significant downfield for C-6 and upfield for C-7 and C-8 relative to compound **6** (98.8 ppm). In contrast, the A ring carbon signals in flavones are markedly affected by the introduction of a methoxy group at 3-position [47]. Accordingly, a deshielding effect of about +34 ppm is found for C-3 in compound **9**, and shielding effect was shown in C-2 and C-4. The remaining carbon resonances of four flavones were completely assigned by comparison with previously reported data [39–42]. Complete acid hydrolysis of compound **7** revealed the presence of aglycone part, which has the same chromatographic character as compound **6**. The sugar moiety was detected by PC along side with authentic sugar and it proved to be glucose. Compound **6**, **7**, **8**, and **9** were identified as lutoelin-3′-methyl ether, luteolin 3′-methyl ether-7-glucoside, 3′,5-dihydroxy-6,7,4′-trimethoxyflavone (luteolin-6,7,4′-trimethyl ether), and 5-hydroxy-

3,6,7,3′,4′-pentamethoxy flavone (artemetin), respectively. The analytical data were in agreement with those reported in the literatures [39–42].

Phytoconstituents of the ethyl acetate and methanol extracts of *A. judaica* is suggested to be responsible for the hypolipidemic and hypoglycemic effect resulting in the detected amelioration in kidney function. The nephroprotective activity may be carried out by enhancing insulin production and decreasing glucagon production in diabetic rats. In agreement with the present work, the hepatoprotetive and nephroprotective actions of essential oil extract of *Artemisia sieberi* in alloxan-induced diabetic rats were reported [48]. In addition, *Chrysanthemum indicum* extract exhibited a promising protective effect on cisplatin-induced nephrotoxicity [21].

In the current study, the biochemical investigation is supported by histopathological examination of kidney in each plant successive extract-treated hyperlipidemic–hyperglycemic rats. The reduction in lipid peroxide and increased antioxidant activities in rats treated with each plant successive extracts may be related to lower lipid accumulation and blood glucose levels that in turn lead to histopathological amelioration. The present study clearly shows that plant extracts may be of therapeutic importance not only as blood glucose and lipid-lowering agents in serum, but also as a cytoprotective agent to protect the kidney from hyperlipidemic and hyperglycemic synergistic effect.

Conclusion

The results suggested that two Asteraceae plants might act as beneficial agents against renal dysfunctions developed in high fat diet (hyperlipidemic) and low dose STZ-induced hyperglycemia. The bioactivity of the most promising extract may be attributed to the terpenoidal and flavonoidal compounds.

Acknowledgements

The authors thank the National Research Centre for funding this research study.

Conflicts of interest

There are no conflicts of interest.

References

1 Ginter E, Simko V. Garlic (*Allium sativum* L.) and cardiovascular diseases. Bratisl Lek Listy 2010; 111:452–456.

2 Loew D, Kaszkin M. Approaching the problem of bioequivalence of herbal medicinal products. Phytother Res 2002; 16:705–711.

3 Anwar MM, Meki AR. Oxidative stress in streptozotocin induced diabetic rats: Effects of garlic oil and melatonin. Comp Biochem Physiol A Mol Integr Physiol 2003; 135:347–539.

4 Abu-Gabal NS, Abd Alla HI, Ahmed HH, Al-Saigh SM, Shalaby NMM. Efficacy of aloe vera extracts in attenuating neurological endangerment-induced by dexamethasone in adult male rats. J Arab Soc Med Res 2007; 2:59–73.

5 Shalaby NMM, Abd-Alla HI, Aly HF, Albalawy MA, Shaker KH, Bouajila J. Preliminary in vitro and in vivo evaluation of antidiabetic activity of Ducrosia anethifolia Boiss and its linear furanocoumarins. BioMed Res Int 2014; 2014:1–13. *http://www.hindawi.com/journals/bmri/aip/480545/*

6 Hu CK, Lee YJ, Colitz CM, Chang CJ, Lin CT. The protective effects of *Lycium barbarum* and *Chrysanthemum morifolum* on diabetic retinopathies in rats. Vet Ophthalmol 2012; 15:65–71.

7 Sefi M, Fetoui H, Soudani N, Chtourou Y, Makni M, Zeghal N. *Artemisia campestris* leaf extract alleviates early diabetic nephropathy in rats by inhibiting protein oxidation and nitric oxide end products. Pathol Res Pract 2012; 208:157–162.

8 Adaramoye OA, Akintayo O, Achem J, Fafunso MA. Lipid-lowering effects of methanolic extract of *Vernonia amygdalina* leaves in rats fed on high cholesterol diet. Vasc Health Risk Manag 2008; 4:235–241.

9 Srinivasan K, Viswanad B, Asrat L, Kaul CL, Ramarao P. Combination of high-fat diet-fed and low-dose streptozotocin-treated rat: a model for type 2 diabetes and pharmacological screening. Pharmacol Res 2005; 52:313–320.

10 Rustaiyan A, Masoudi S. Chemical constituents and biological activities of Iranian Artemisia species. Phytochem Lett 2011; 4:440–447.

11 Lei YF, Chen JL, Wei H, Xiong CM, Zhang YH, Ruan JL. Hypolipidemic and anti-inflammatory properties of Abacopterin A from *Abacopteris penangiana* in high-fat diet-induced hyperlipidemia mice. Food Chem Toxicol 2011; 49:3206–3210.

12 Andrade-Cetto A, Wiedenfeld H. Hypoglycemic effect of *Acosmium panamense* bark on streptozotocin diabetic rats. J Ethnopharmacol 2004; 90:217–220.

13 Schirmeister J. Determination method of creatinine. Dtsch Med Wschr 1964; 89:1940–1947.

14 Fawcett JK, Scott JE. Determination method of total urea. J Clin Pathol 1960; 13:156–159.

15 Wood JL. Biochemistry of mercapturic acid formation. In: Fishman WHed. *Metabolic conjugation and metabolic hydrolysis*. New York: Academic Press; 1970. 2:261–299.

16 Allen BW, Liu J, Piantadosi CA. Electrochemical detection of nitric oxide in biological fluids methods in enzymology. Methods Enzymol 2005; 396:68–77.

17 Suzuki H, Suzuki K. Rat hypoplastic kidney (hpk/hpk) induces renal anemia, hyperparathyroidism, and osteodystrophy at the end stage of renal failure. J Vet Med Sci 1998; 60:1051–1058.

18 McCue P, Horii A, Shetty K. Solid-state bioconversion of phenolic antioxidants from defatted soybean powders by *Rhizopus oligosporus*: role of carbohydrate-cleaving enzymes. J Food Biochem 2003; 27:501–514.

19 Katsube T, Tabata H, Ohta Y, Yamasaki Y, Anuurad E, Shiwaku K, Yamane Y. Screening for the antioxidant activity in edible plant products: comparison of low-density lipoprotein oxidation assay, DPPH radical scavenging assay, and Folin–Ciocalteu assay. J Agric Food Chem 2004; 52:2391–2396.

20 Huang TH, Kota BP, Razmovski V, Roufogalis BD. Herbal or natural medicines as modulators of peroxisome proliferator-activated receptors and related nuclear receptors for therapy of metabolic syndrome. Basic Clin Pharmacol Toxicol 2005; 96:3–14.

21 Pongjit K, Ninsontia C, Chaotham C, Chanvorachote P. Protective effect of Glycine max and *Chrysanthemum indicum* extracts against cisplatin-induced renal epithelial cell death. Hum Exp Toxicol 2011; 30:1931–1944.

22 Wurochekke AU, Anthony AE, Obidah W. Biochemical effects on the liver and kidney of rats administered aqueous stem bark extract of *Xemenia americana*. Afr J Biotechnol 2008; 7:2777–2780.

23 Montilla P, Barcos M, Munoz MC, Bujalance I, Munoz-Castaneda JR, Tunez I. Red wine prevents brain oxidative stress and nephropathy in streptozotocin-induced diabetic rats. J Biochem Mol Biol 2005; 38:539–544.

24 Eddy AA, Lui E, McCulloch L. Interstitial fibrosis in hypercholesterolemic rats: role of oxidation matrix synthesis, and proteolytic cascades. Kidney Int 1998; 53:1182–1189.

25 Gauci S, Helbig AO, Slijper M, Krijgsveld J, Heck AJ, Mohammed S. Lys-N and trypsin cover complementary parts of the phosphoproteome in a refined SCX-based approach. Anal Chem 2009; 81:4493–4501.

26 Grune T, Davies KJ. The proteasomal system and HNE-modified proteins. Mol Aspects Med 2003; 24:195–204.

27 Szkudelski T. The mechanism of alloxan and streptozotocin action in B cells of the rat pancreas. Physiol Res 2001; 50:537–546.

28 Arkkila PE, Koskinen PJ, Kantola IM, Ronnemaa T, Seppanen E, Viikari JS. Diabetic complications are associated with liver enzyme activities in people with type I diabetes. Diabetes Res Clin Pract 2001; 52:113–118.

29 Ridker PM, Danielson E, Fonseca FA, Genest J, Gotto AM, Kastelein JJ, *et al.* Reduction in C-reactive protein and LDL cholesterol and cardiovascular event rates after initiation of rosuvastin: a prospective study of the JUPITER trial. Lancet 2009; 373:1175–1182.

30 Lahera V, Goicoechea M, de Vinuesa SG, Miana M, de las HN, Cachofeiro V, Luno J. Endothelial dysfunction, oxidative stress and inflammation in atherosclerosis: beneficial effects of statins. Curr Med Chem 2007; 14:243–248.

31 Harrison DG. Endothelial function and oxidant stress. Clin Cardiol 1997; 20:II-11–II-17.

32 Serounge C, Felgines C, Ferezon J, Hajri T, Bertin C, Mazur A. Hypercholesterolemia induced by cholesterol or cystiene enriched diet is characterized by different plasma lipoprotein and apoproteins concentration in rats. J Nutr 1995; 125:619–623.

33 Abad MJ, Bedoya LM, Apaza L, Bermejo P. The Artemisia L. genus: a review of bioactive essential oils. Molecules 2012; 17:2542–2566.

34 Yoshihiro C, Hiroshi O, Mayumi OK, Tadahiro N, Tojiro T. Structural identification of two antioxidant quinic acid derivatives from garland (*Chrysanthemum coronarium* L). J Agric Food Chem 1996; 44:2037–2039.

35 Abd-Alla HI, Albalawy MA, Aly HF, Shalaby NMM, Shaker KH. Flavone composition and antihypercholesterolemic and antihyperglycemic activities of *Chrysanthemum coronarium* L. Z Naturforsch 2014; 69c. in press

36 Kim JS, Ju JB, Choi CW, Kim SC. Hypoglycemic and antihyperlipidemic effect of four Korean medicinal plants in alloxan induced diabetic rats. Am J Biochem Biotechnol 2006; 2:154–160.

37 Hudaib MM, Tawaha KA, Mohammad MK, Assaf AM, Issa AY, Alali FQ, *et al.* Xanthine oxidase inhibitory activity of the methanolic extracts of selected Jordanian medicinal plants. Pharmacogn Mag 2011; 7:320–324.

38 Xia DZ, Lv GY, Yu XF, Wang HM, Yang Q. Antagonism of total flavonoids from *Chrysanthemum morifolium* against lead induced oxidative injury in mice. Zhongguo Zhong Yao Za Zhi 2008; 33:2803–2808.

39 Mabry TJ, Markham KR, Thomas MB. *The systematic identification of flavonoids*. Berlin: Springer-Verlag; 1970. 41–164.

40 Harborne JB, Mabry TJ. *The flavonoids: advances in researches, Chapter 2.* London: Chapman and Hall Ltd; 1982.

41 Saleh NAM, El-Negoumy SI, Bou-Zaid MM. Falvonoids of *Artemisia judaica*, *A. monosperma* and *A. herba-alba*. Phytochemistry 1987; 26:3059–3064.

42 Elgamal MHA, Ouf SA, Hanna AG, Yassin FY. Phytochemical and mycological investigation of *Artemisia monosperma*. Folia Microbiol 1997; 42:203–210.

43 Goad LJ, Akihisa T. *Analysis of sterols*. 1st ed. London, New York, Tokyo, Melbourne, Madras: Blackie Academic and Professional, an imprint of Chapman and Hall; 1997.

44 Koul S, Razdan TK, Andotra CS, Kalla AK, Koul S, Taneja SC, Dhar KL. Koelpinin-A, B and C-three triterpenoids from *Koelpinia linearis*. Phytochemistry 2000; 53:305–309.

45 Gearien JE, Bauer L, Klein M, Levine B. Structure of lupeol and its 19alpha-H-isomer. J Pharm Sci 1975; 64:152–154.

46 Park Y, Moon BH, Yang H, Lee Y, Lee E, Lim Y. Complete assignments of NMR data of 13 hydroxymethoxyflavones. Magn Reson Chem 2007; 45:1072–1075.

47 Markham KR. *Techniques of flavonoids identification*. London: Academic Press; 1982.

48 Irshaid F, Mansi K, Bani-Khaled A, AburjiT. Hepatoprotetive, cardioprotective and nephroprotective actions of essential oil extract of *Artemisia sieberi* in alloxan induced diabetic rats. Int Conf Chem Environ Biol Sci 2011; 362–367.